
Film Cooling Effectiveness from Single and Two Inlined/ Staggered Rows of Novel Semicircular Cooling Holes

FAYYAZ HUSSAIN ASGHAR*, AND MUHAMMAD JAVED HYDER*

RECEIVED ON 10.06.2009 ACCEPTED ON 18.11.2009

ABSTRACT

Computational analysis of film cooling effectiveness using novel semicircular hole shapes with streamwise inclination of 30° has been carried out. Pitch to diameter ratios of 3.0 has been investigated. Reynolds Averaged Navier-Stoke equation solver FLUENT with standard k- turbulence model is used for simulations. Coolant to mainstream blowing ratios is varied from 1.33-2.0. It is observed that for the streamwise region $x/D < 20$ the centerline and laterally averaged effectiveness values from a row of semicircular holes are higher than that from a row of circular holes due to the less jet lift-off of coolant jet. For a row of semicircular holes, mean coolant jet heights are lower than that from a row of circular holes. Simulations for two rows of inlined and staggered semicircular holes are also carried out and the results are compared with single row of full circular holes. It is found that centerline and laterally averaged effectiveness values from 2 rows of semicircular holes are much higher than a single row of full circular hole case at all streamwise regions at all blowing ratios tested. Among all the cases studied, effectiveness values from two staggered rows of semicircular holes are found to be highest. Jet lift-off is found minimum from two staggered row of semicircular holes. For all cases studied, the mean coolant jet heights from two staggered rows of semicircular holes are found minimum. Results for counter rotating vortex pairs from all cases at plane normal to mainstream flow have also been analyzed.

Key Words: CFD, Film Cooling Effectiveness, Heat Transfer, Fluid Flow, Turbine Blade Cooling.

1. INTRODUCTION

To achieve higher turbine efficiency in the form of increased thrust and power output, higher temperatures at the combustion chamber outlet (turbine inlet) are needed. However, these higher temperatures threaten the structural integrity of turbine components. To keep the temperature of turbine components below allowable limits, cooling is required. Film cooling is one technique, which has being used widely in present high temperature gas turbine engines apart from thermal barrier coating methods.

In film cooling method relatively cool air taken from last stage of compressor is fed into internal chambers of turbine blades and ejected out through small holes to spread on the surface of turbine blade. This air protects the components from incoming hot fluid by making a layer of cool air on the surface.

Film cooling effectiveness (η) is used to express the film cooling phenomena quantitatively. As film cooling experimental studies are usually conducted on an adiabatic flat plate [1] so η in that case is called as adiabatic film cooling effectiveness.

* Pakistan Institute of Engineering and Applied Sciences (PIEAS), Nilore, Islamabad, Pakistan.

$$\eta = \frac{T_{aw} - T_{\infty}}{T_c - T_{\infty}} \quad (1)$$

Where T_{aw} is adiabatic wall temperature, T_c is coolant inlet temperature, and T_{∞} = mainstream inlet temperature.

Non-dimensional temperature (θ) of fluid [2] at temperature T is defined here in the similar manner.

$$\theta = \frac{T - T_{\infty}}{T_c - T_{\infty}} \quad (2)$$

Film cooling effectiveness depends on many parameters like cooling hole shape, cooling hole inclination, arrangement of row of holes, properties of mainstream fluid, coolant to mainstream blowing ratios, density ratio and velocity ratios.

Film cooling flows are typical case of jet in a crossflow, these flows are dominated by complex flow structures like counter rotating vortex pairs, so there is a continuous need of understanding the physics of film cooling flows and their effect on film cooling effectiveness.

Film cooling effectiveness using a single cylindrical hole and a row of holes at streamwise angle of 30, 60, and 90° is studied by Yuen, et. al. [1,3]. Experimental study to present the flow structure for flat plate film cooling is performed by Bernsdorf, et. al. [4]. Flow structures for different blowing ratios are presented and decrease of boundary layer thickness is found with increasing blowing ratio. It is proposed that increase in heat transfer coefficient with increasing blowing ratio is associated with this decrease of boundary layer thickness.

Guo, et. al. [5] numerically investigated the mean velocity and turbulent kinetic energy fields for lateral jet in crossflow at injection angle of -60 and -30°. The RNG k-model with two-layer wall function method is used for turbulence modeling. Separation events are found in the lee of the jet exit and behind the jet. Investigations of the effect of coolant to free-stream velocity ratios on film cooling effectiveness under gas turbine engine like

conditions are presented by Hyder, et. al. [6]. Velocity ratio of 0.2 is found best among the velocity ratio range of 0.1-1.0. Wang, et. al. [7] used commercial software FLUENT to study the effect of injecting a small amount of water into the cooling air for film cooling performance. Simulations are conducted at gas turbine operating conditions like the mainstream flow was at 15 atm with a temperature of 1561 K. It is found that 10-20% mist achieved 5-10% cooling enhancement.

Influence of different hole shapes on film cooling with CO₂ injection are investigated by Li, et. al. [8]. They investigated simple cylindrical holes, 3-in-1 holes and fanned holes. In terms of film cooling performance, the fanned holes are found best while the simple cylindrical holes are the worst among the three hole shapes. An experimental study is conducted by Yang, et. al. [9] for film cooling performance and heat transfer over an inclined film cooled surface at different divergent angles (0-20°). Mixing of the film jet with free-stream is found increasing with increase in free-stream turbulence intensity. Increasing the divergent angle of the film cooled surface also resulted in enhanced mixing of the film jet with free-stream.

Large eddy simulations are used by Rozati, et. al. [10] to investigate the effect of coolant-mainstream blowing ratio on leading edge film cooling flow and heat transfer. They found decrease in adiabatic effectiveness with an increase in blowing ratio due to the increased mixing between coolant jet and the mainstream. Lee, et. al. [11] investigated the jet flows through a row of forward expanded holes into a mainstream over a concave surface. 2D mean velocity maps on several horizontal and vertical planes; and a 3D streamline pattern of jet mean velocity are presented. Jovanovic, et. al. [12] investigated the effect of hole imperfection on adiabatic film cooling effectiveness. Half torus inside the cooling hole is used as a discrete imperfection. Imperfection placed one diameter from the hole leading edge is found to deteriorate the effectiveness while the same imperfection fixed at the hole exit improved the effectiveness.

Pathak, et. al. [13] used $k-\epsilon$ turbulence model to simulate the mean flow field of turbulent rectangular jets issuing into a narrow channel crossflow. The effect of turbulent Prandtl number on the computation of film cooling effectiveness is investigated by Liu, et. al. [14] and increase in film cooling effectiveness of whole spanwise region under large blowing ratios and reduced Prandtl number is found. Under small blowing ratios, the reduction of turbulent Prandtl number is found to decrease the cooling effectiveness of the center region and to increase the effectiveness of the lateral region off the centerline. A new laterally varying turbulent Prandtl number model dependent on the lateral location and blowing ratio is suggested by Lie, et. al. [14].

Effect of coolant to free-stream blowing ratios and boundary layer thickness on adiabatic film cooling effectiveness is investigated by Asghar, et. al. [15]. Highest value of two-dimensionally-averaged effectiveness is found at a blowing ratio of 1.0. Asghar, et. al., [16] further conducted the computational study for comparison of cylindrical, square and triangular hole shapes of equal cross-sectional area, triangular hole having lateral straight edge on windward side and converging corner on leeward side is found to show lesser coolant jet height and higher film cooling effectiveness in the region $x/D > 10$, especially at blowing ratios greater than 1.0. In experiment by Yang, et. al. [17] the adiabatic wall film cooling effectiveness is studied over a film cooled surface that was made inclined at various angles with respect to highly turbulent flow. Increased mixing of film jet and hence decreased film cooling effectiveness is found with increasing turbulent intensity and convergent angle of the film cooling surface.

Our objective is to work out the different geometrical shapes of cooling holes to achieve higher cooling effectiveness. At present shaped holes are found to give best cooling effectiveness. But shaped holes are constructed from the shaping of simple cylindrical holes.

However, new hole shapes should also be tested in comparison with simple cylindrical holes. In the present study, effectiveness from rows of semicircular holes is compared with row of cylindrical hole case. Motivation behind this work is due to the fact that semicircular holes utilize half of the blade volume as compare to full cylindrical holes, thus giving more structural strength to blade. Also semicircular holes required half mass flow rate of coolant to achieve the same blowing ratio as in case of cylindrical holes. Hence in present work computational study has been conducted to understand the film cooling flows with a single row and two rows (staggered/inlined) of streamwise inclined semicircular holes with 30° streamwise angle of injection. Pitch to diameter ratio (p/D) used is 3.0.

2. METHODOLOGY

In the first part of present study, the experimental study of Yuen, et. al. [1] is used as a benchmark test case to compare the results of a row of circular cooling hole with streamwise injection angle of 30° and pitch to diameter ratio of 3.0 ($p/D=3.0$). A cross-sectional view (as seen from z-direction) of the geometrical model is shown in Fig. 1, while Fig. 2 shows top (as seen from y-direction) view of test plate for different case studied. Four geometric cases have been studied. First is the baseline case of single row of circular holes with pitch to diameter ratio of 3.0, which is used for validation of computational model. Second is the case of a single row of semicircular holes with pitch to diameter ratio of 3.0. Third is the case of 2 inline rows of semicircular holes with row spacing of $3.0D$. Fourth is the case of two staggered rows of semicircular holes separated by $3.0D$ streamwise distance and the lateral separation between two neighboring holes from different rows is $1.5D$ while lateral separation between holes of individual row is $3D$. Fig. 3 shows the selection of geometrical domain due to symmetry of the problem. The exact dimensions and parameters have been chosen so that the results of single row of holes can be compared with the benchmark experimental results.

An adiabatic wall boundary condition is used at all boundaries except those denoted as "main inlet", "coolant inlet", "outlet" in Fig. 1, and symmetry boundary conditions are applied at symmetry planes $z/D=0.0$ and $z/D=p/2=1.5$ (Fig. 3). At the "main inlet," a velocity-inlet

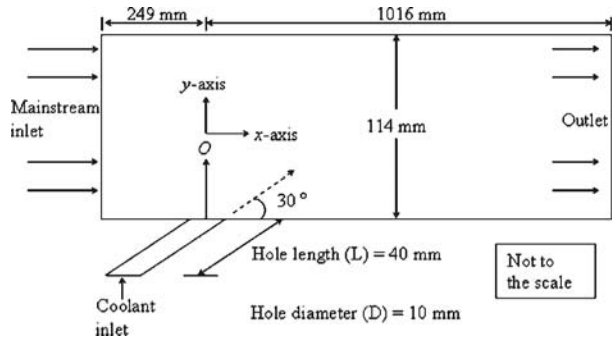


FIG. 1. CROSS-SECTIONAL VIEW OF GEOMETRY AT yz-PLANE ($z=0.0$)

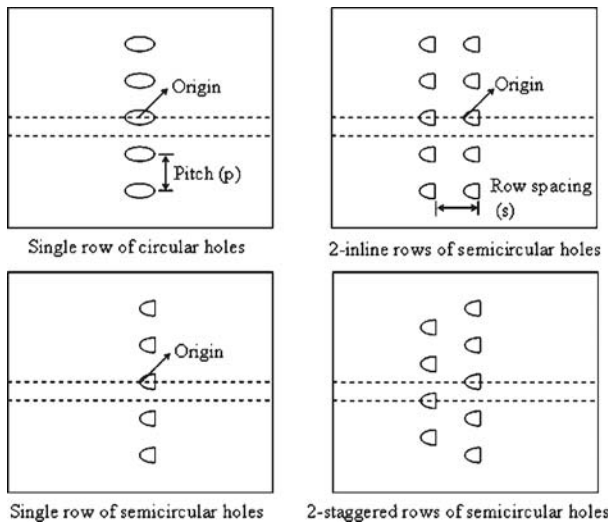


FIG. 2. ARRANGEMENT OF HOLES FOR DIFFERENT CASES

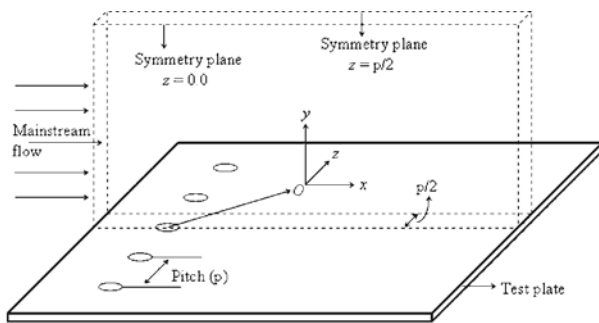


FIG. 3. SYMMETRY PLANES IN COMPUTATIONAL DOMAIN

boundary condition is specified with x-velocity equal to 13m/s and all other components equal to zero. The temperature is given as 293.15K at the main inlet. The turbulence intensity and hydraulic diameter (which is used to determine turbulence length scales) are specified as 2.7% and 26.51mm, respectively. At the "coolant inlet," a velocity-inlet boundary condition is varied from case to case as specified in Table 1. The temperature of the coolant is 318.15K to match the coolant to free-stream density ratio of 0.92 with experiment of Yuen, et. al. [3]. For the coolant, the turbulence intensity and hydraulic diameter are specified as 3% and 5mm, respectively. At the "outlet", a pressure-outlet boundary condition is specified with gage pressure equal to 0 (giving an absolute pressure of 101,325 Pa). Reynolds number based on free-stream velocity and hole diameter is 10364. For the case of without film cooling hole, at $x/D=0.0$, the velocity boundary layer thickness is $\delta=0.72D$, displacement thickness is $\delta^*=0.23D$ and momentum thickness is $\delta_i=0.17D$, Blowing ratios ranging from 1.33-2 have been investigated.

2.2 Grid Generation

Computational domain selected for the simulations is shown in Fig. 3, where $z/D=0.0$ and $z/D=p/2=1.5$ are the symmetry planes. For multi-block grid generation, GAMBIT is used. Meshing for mainstream duct is same for the cases of semicircular and circular holes. Grid independent study has been performed for circular hole case at the blowing ratio of $M=1.33$. Fig. 4 shows the grid independent study for non-dimensional velocity profile and non-dimensional temperature (ϕ) profile respectively, for $x/D=10$, and $z/D=0.0$, it is clear that the results in case of medium and fine meshes are almost similar and solution becomes mesh independent after medium mesh. Hence

TABLE 1. PLENUM INLET VELOCITIES

Case No.	Blowing Ratio		
	(M)	VR	V_c (m/sec)
1.	1.33	1.444	18.772
2.	1.67	1.813	23.569
3.	2.0	2.171	28.223

medium mesh is used for CFD simulation. Table 2 shows the grid sizes for different meshes. After selection of final meshing scheme from grid independent study of row of cylindrical holes, same meshing scheme is used for mainstream duct geometry for all cases of semicircular and circular holes. Only difference in meshes is where the hole shape are different.

2.2 Solver

For CFD simulations FLUENT 6.2.12 is used. Depending on the nature of the problem (i.e. 3D steady state problem with low velocity values) 3D segregated, steady state solver is used. Coupled solver is recommended for sonic and supersonic velocities while for low velocities segregated solver should be used, FLUENT [18]. For

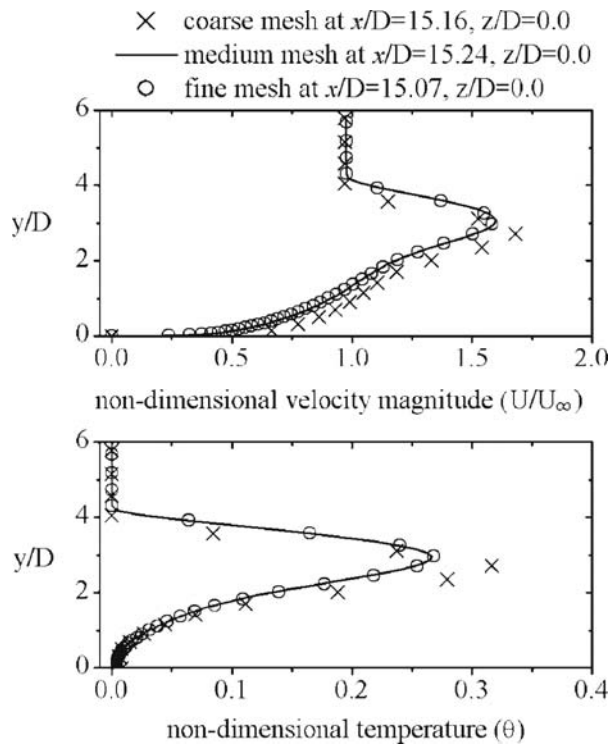


FIG. 4. MESH INDEPENDENCY

TABLE 2. GRID SIZES FOR DIFFERENT MESHES

	Coarse	Medium	Fine
Cells	49273	346773	677173
Faces	147340	1057177	2055572
Nodes	49824	364485	701757

linearization of governing equations implicit method is used. For turbulence modeling k-ε model with standard wall functions of , Launder, et. al. [19] is used as recommended by Zhang, et. al. [20] for film cooling study. To avoid use of enhanced wall treatment mesh was kept fine enough to have wall Y+ in the range 0-5.

Discretization scheme used is 2nd order upwind by Barth, et. al. [21] for momentum, turbulence kinetic energy, turbulence dissipation rate and energy, whereas for pressure standard discretization scheme by Rhie, et. al. [22] is used. For pressure-velocity coupling SIMPLE algorithm of Patankar, et. al. [23] is used.

3. RESULTS AND DISCUSSION

For validation purpose of CFD model, present computational results of centerline effectiveness (η_c) for blowing ratios of M=1.33 and M=1.67 are compared with experimental results of Yuen, et. al., [3] for pitch to diameter ratio (p/D) of 3.0 and hole streamwise inclination of 30° (Fig. 5). Computational results are well in agreement with experimental results except in near hole region (x/D<3), where centerline adiabatic effectiveness is over predicted. However, for most of the streamwise region (3<x/D<100), the computational results are in excellent agreement with experimental results, which validates the computational model used.

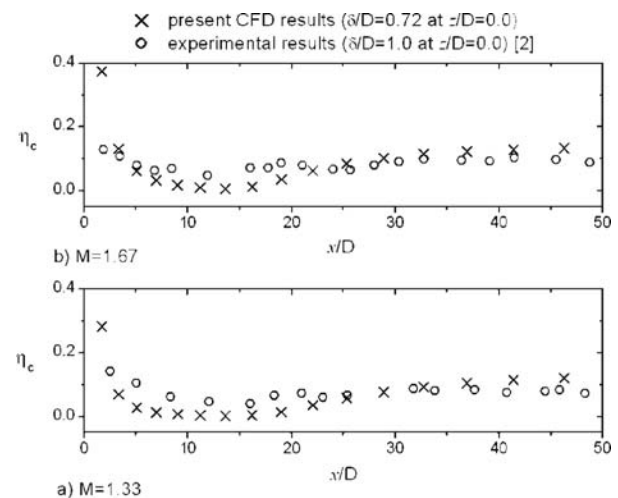


FIG. 5. COMPARISON WITH EXPERIMENTAL RESULTS

Fig. 6 shows the comparison of centerline effectiveness from a row of circular holes and a row of semicircular holes for three different blowing ratios of 1.33, 1.67 and 2.0. It is found that centerline effectiveness from a row of semicircular holes have comparatively higher values in the region $x/D < 20.0$ as compare to values from a row of circular holes. Higher values of centerline effectiveness from a row of semicircular holes in the region $x/D < 20.0$ is due to less jet lift-off as compare to jet lift-off from a row of circular holes. Less jet lift-off keeps the coolant jet more towards test wall and hence shows higher effectiveness values. After the region $x/D > 20.0$, centerline effectiveness values from a row of circular holes have higher values than that from a row of semicircular holes. This is due the coming back of coolant jet towards test plate, which was lifted more in the region $x/D < 20.0$ for the row of circular hole case. However, in the region $x/D > 20.0$, the difference in effectiveness between two cases is very small.

Comparison of laterally averaged effectiveness ($\bar{\eta}$) from a row of circular holes and from a row of semicircular holes is shown in Fig. 7 for three different blowing ratios

($M=1.33, 1.67, 2.0$). For blowing ratio of $M=1.33$ (Fig. 7(a)), values are higher for the case of row of semicircular holes in the region $x/D < 20.0$, however after streamwise region of $x/D > 20.0$, $\bar{\eta}$ values are higher for the case of row of circular holes showing more lateral spread of coolant in that region. Increase in effectiveness after early decrease is due to the jet reattachment. The jet reattachment region for a row of semicircular holes is farther than that from a row of circular holes, which is the cause of lower effectiveness values from a row of semicircular holes after $x/D > 20$, however, the difference is small between the two cases.

Same or higher values of effectiveness from a row of semicircular holes as compare to a row of circular holes are advantageous in many ways. First semicircular holes occupy only half of the blade volume as compare to circular holes, hence can provide more structural strength to turbine blade. Second semicircular hole requires half mass flow rates than that required for circular holes; hence it indirectly increased the thermal efficiency of gas turbine. To keep the total mass flow of coolant same, simulations have also been performed for two rows of

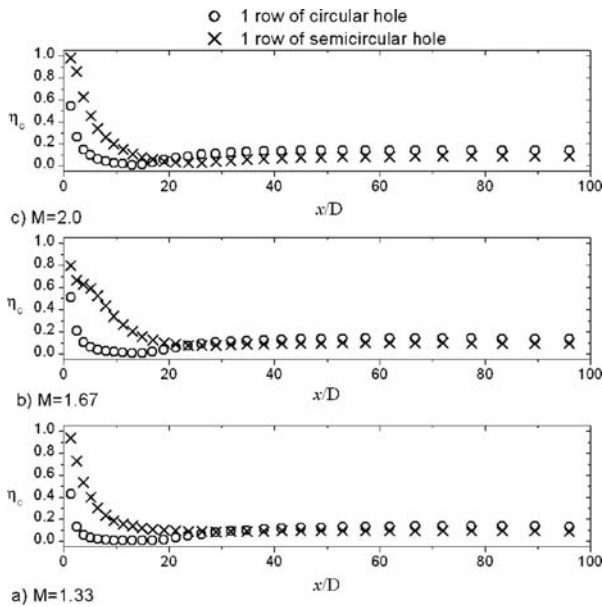


FIG. 6. CENTERLINE EFFECTIVENESS FOR SINGLE ROW OF HOLES

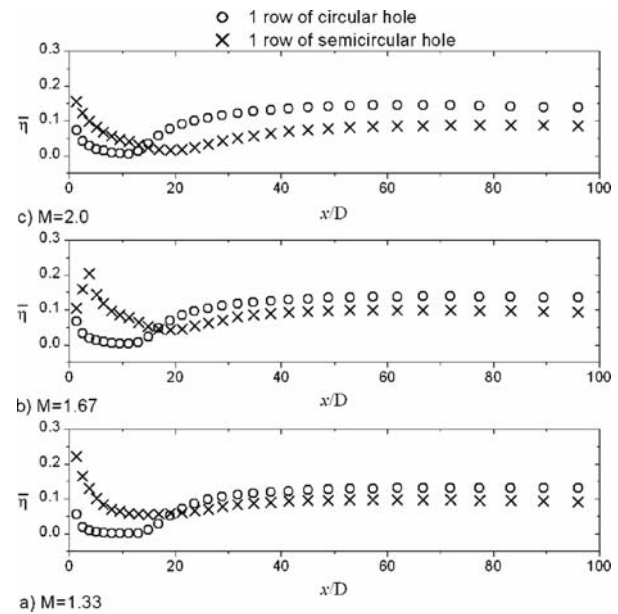


FIG. 7. LATERALLY AVERAGED EFFECTIVENESS FOR SINGLE ROW OF HOLES

semicircular holes. Fig. 8 shows the centerline effectiveness comparison of single row of circular hole with two inline rows and two staggered rows ($s/D=3.0$) of semicircular holes. Centerline effectiveness values (Fig. 8) from both inline and staggered rows of semicircular holes are found to be much higher than the values from a single row of circular holes at all x/D values and at all blowing ratios ($M=1.33, 1.67, \text{ and } 2.0$). Among the two rows of semicircular holes, inline rows of semicircular holes only show higher effectiveness than staggered rows in the region $x/D < 10$ and for blowing ratios $M=1.33$ (Fig. 8(a)) and $M=1.67$ (Fig. 8(b)). The reason is that the coolant from downstream row of semicircular holes is supported by the coolant from upstream row of holes. In the streamwise region $x/D < 10$ at blowing of $M=2.0$ both cases of two rows of semicircular holes show almost similar results (Fig. 8(c)). After the region $x/D > 10$, the staggered rows of semicircular holes shows higher effectiveness than the inline rows of semicircular holes at all blowing ratios, since the staggered rows of semicircular holes gives a wide spread of coolant on the surface and hence the low room for mainstream flow to enter in between the neighboring holes of downstream row.

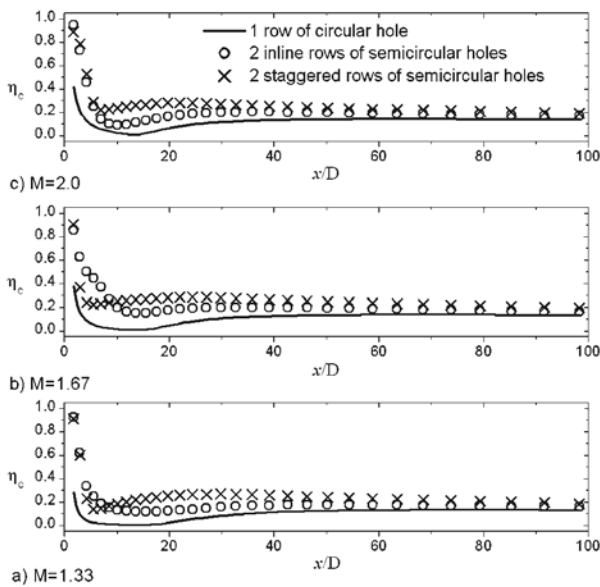


FIG. 8. CENTERLINE EFFECTIVENESS FROM 2 ROWS OF SEMICIRCULAR HOLES

Fig. 9 shows the comparison of laterally averaged effectiveness (lateral average is taken over the lateral distance of $0 < z/D < 1.5$) from two rows of semicircular holes with a single row of circular holes. Here it is found that at all blowing ratios tested and at all streamwise distances, lateral spread of coolant from both inline and staggered rows of semicircular holes is much higher than that from single row of circular hole as can be observed by higher effectiveness values (Fig. 9) from 2 rows of semicircular holes. Among inlined and staggered row of semicircular holes, staggered rows shows more lateral distribution of coolant as compare to inlined rows case. Along streamwise distance, increase of effectiveness after early decreasing trend is due to the reattachment of the coolant jet to the test surface. An early reattachment of coolant jet is seen for the case of staggered rows as compare to inlined rows. Reason for this is the reduction of free space for mainstream flow to surround the coolant jet. Also for the staggered rows of holes area downstream of holes is doubled, which is also the reason for higher effectiveness values.

Fig. 10 shows the overall averaged effectiveness over the region $0.0 < z/D < 1.5, 1.6 < x/D < 100$, for all cases. It is clear

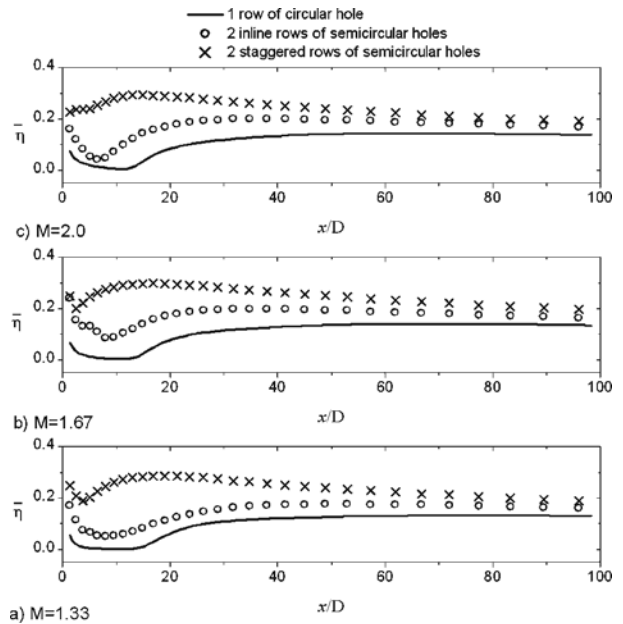


FIG. 9. LATERALLY AVERAGED EFFECTIVENESS FROM 2 ROWS OF SEMICIRCULAR HOLES

that overall two dimensional averaged from a single row of circular or semicircular holes are almost similar. Reason is explained earlier that semicircular holes are found to exhibit lower jet heights and keep the coolant towards test plate. However, lesser coolant mass is available for semicircular holes to spread out on the test plate, so this will reduce the effectiveness. Combination of both of these effects resulted in almost similar values of 2D averaged effectiveness from a row of circular holes and a row of semicircular holes. Two inlined and staggered rows of semicircular holes show much higher values of overall averaged effectiveness as compare to that from a single row of circular holes case. Among all cases, staggered rows of semicircular holes show best performance.

Fig. 11 shows the non-dimensional temperature (θ) profiles at center-plane $z/D=0.0$ and at streamwise location $x/D=10$. Mainstream fluid has $\theta=0.0$ as non dimensional temperature, while coolant has $\theta=1.0$ as non dimensional temperature. Mean jet height at particular location is determined by maximum θ -value at that location. It is seen that with increasing blowing ratio coolant jet height increases which is clear from increasing y/D distance with increasing blowing ratio to reach maximum θ -value. Also coolant jets heights from all cases of semicircular holes are much lower than the coolant jet heights from the row of circular cooling holes. It is a great advantage; because

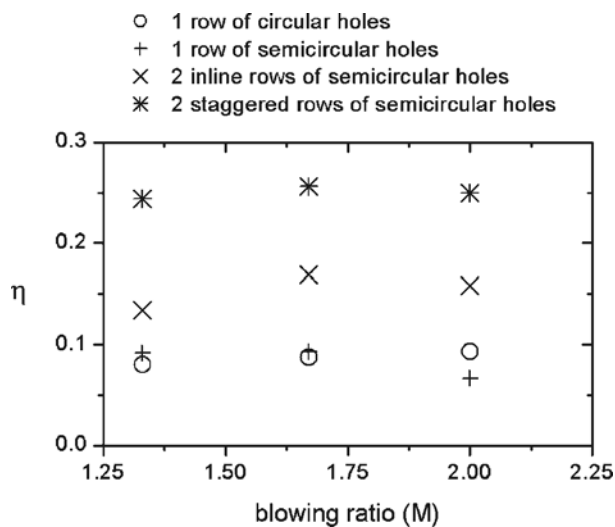


FIG. 10. OVERALL AVERAGE EFFECTIVENESS

along with more cooling of test plate it is also required that coolant mixing with the mainstream fluid should be as less as possible. Among all the cases studied, the minimum coolant jet heights are found for two staggered rows of semicircular (Fig. 11). It is also found that in the near wall region (at low y/D values), the coolant presence is more from semicircular hole cases (single row or two rows) as compare to single row of circular holes, which is clear from the higher θ -values (Fig. 11) from semicircular hole cases in the near wall region at all blowing ratio tested, which is also the reason for higher effectiveness from semicircular holes cases as seen in Figs. 8-9.

Fig. 12 shows the θ -profiles at center-plane $z/D=0.0$ and at streamwise location of $x/D=20$. Results are almost similar as seen at the streamwise location of $x/D=10$, except the absence of peak in θ -values for the case of two staggered rows of semicircular holes. The peak in θ -values is actually shifted towards the near wall region ($y/D \sim 0.0$) showing the re-attachment of coolant jet with the test.

Fig. 13 shows the velocity vectors at plane $x/D=10.0$ normal to the mainstream flow at blowing ratio of 1.33. The velocity vectors are colored by non-dimensional temperature (θ).

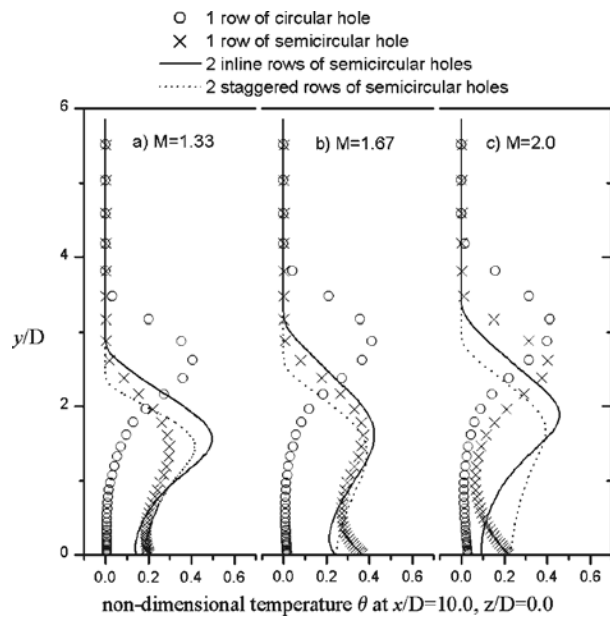


FIG. 11. NON-DIMENSIONAL TEMPERATURE PROFILES AT $x/D=10$

The counter rotating vortex pairs are clear. These counter rotating vortex pairs increases the jet height and causes the mainstream to entrain into the coolant jet. It is clear from Fig. 13 that the center of counter rotating vortex pairs from a single row of circular hole case is higher (at approximately $y/D=1.5$) than that from other cases. Also the strength of counter rotating measured by the magnitude of velocity vectors is higher for single row of circular holes than that from the single row of semicircular holes or from the two staggered rows of semicircular holes, however the strength of counter rotating vortex pair from two inlined rows of semicircular holes is found to be highest. It can also be seen that more mainstream fluid enter below the counter rotating vortex pair for the case of circular holes than other cases as clear from the blue velocity vectors ($\theta \sim 0.0$) in that case which represents the mainstream fluid. The weakest velocity vectors in the counter rotating vortex pairs are found for the case of two staggered rows of semicircular holes case, which is the main reason for highest effectiveness results (Fig. 9) for that case.

Fig. 14 shows the non-dimensional temperature contours on the plane $x/D=10.0$ normal to mainstream flow. Here it can be seen that for the single row of circular holes the jet

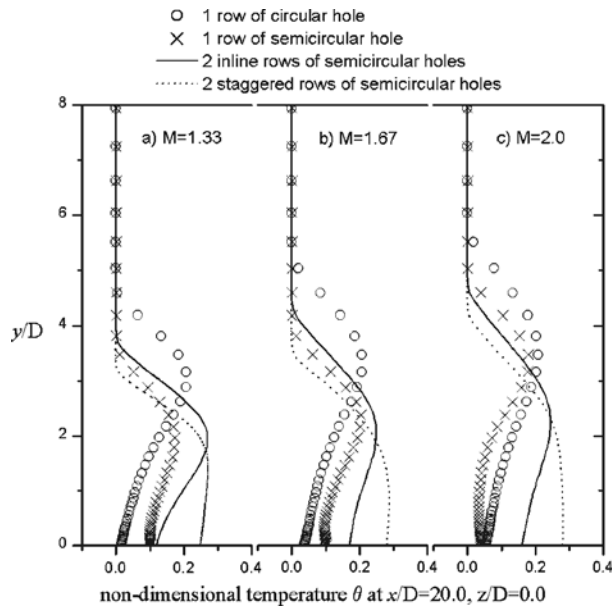


FIG. 12. NON-DIMENSIONAL TEMPERATURE PROFILES AT $x/D=20$

is completely lifted off the test surface and below the coolant jet the mainstream fluid dominates. However, for the cases of single row of semicircular holes and two rows of semicircular holes coolant is also seen to be present near the wall. Coolant dominance in the near wall region (at low y/D values) is found maximum from two staggered rows of semicircular holes, which is the main reason for high effectiveness values for that case.

4. CONCLUSIONS

- (i) Benchmark experimental work for circular film cooling hole with $p/D=3.0$ case and blowing ratios of 1.33 and 1.67 is successfully modeled with results showing good qualitative agreement with the experimental work, although simplest form of 2-equation Reynolds Averaged Navier Stokes solver is used.
- (ii) All pertinent flow structures like jet lift-off, reattachment, and counter rotating vortex pair are observed.
- (iii) Both centerline and laterally averaged film cooling effectiveness from a row of semicircular holes is found higher than that from a row of circular holes for non-dimensional streamwise region $x/D < 20$, after that streamwise region the difference between the effectiveness values from the two cases is found to be very small.
- (iv) Reattachment of coolant jet from a row of circular holes starts after $x/D=15$ while that from a row of semicircular holes starts after $x/D=20$.
- (v) Mean height of coolant jet is found from semicircular holes are found smaller than that from the row of circular holes.
- (vi) Two staggered rows of semicircular holes provide much higher effectiveness values than the one row of circular holes.
- (vii) Minimum coolant jet heights are found for two staggered rows of semicircular holes, also the counter rotating vortex for that case are the weakest one.

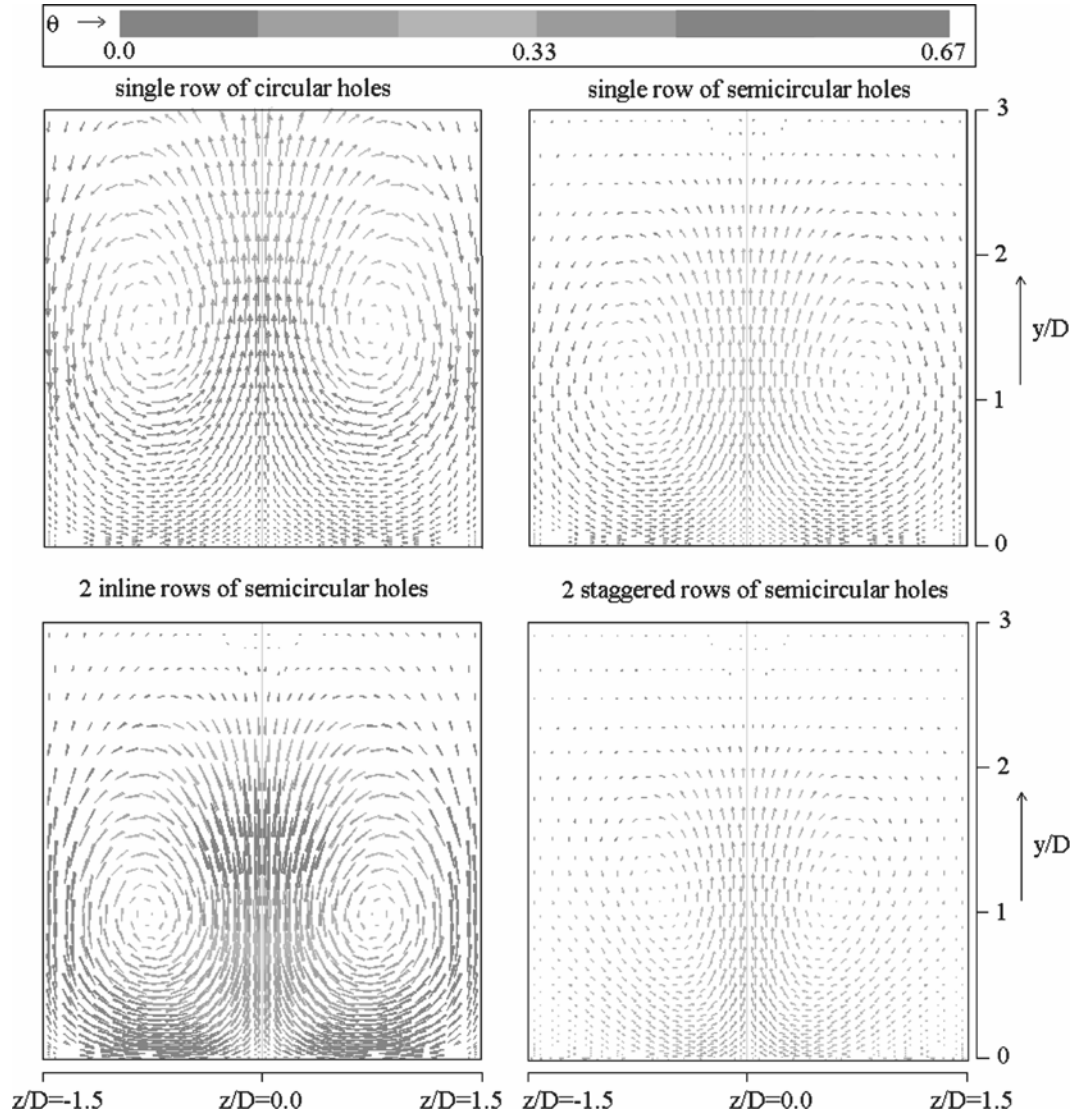


FIG. 13. VELOCITY VECTORS ON $X/D=10.0$ PLANE FOR DIFFERENT CASES AT $M=1.33$

5. NOMENCLATURE

DR	Coolant to Free-Stream Density Ratio
VR	Coolant to Free-Stream Velocity Ratio
M	Coolant-to-Free-Stream Blowing Ratio = $DR \times VR$
D	Diameter of Film Cooling Hole (10mm)
U	Fluid Velocity Magnitude
U_∞	Mainstream Inlet Velocity Magnitude
V_c	Coolant Inlet Velocity Magnitude

Re_D	Reynolds Number Based on Hole diameter and mainstream velocity
x/D	Non-Dimensional Streamwise Distance
y/D	Non-Dimensional Vertical Distance
η	Local Film Cooling Adiabatic Effectiveness
η_c	Centerline Film Cooling Adiabatic effectiveness
$\hat{\eta}_c$	Laterally Averaged Film Cooling Adiabatic Effectiveness ($0.0 < z/D < 1.5$)
T	Fluid Temperature

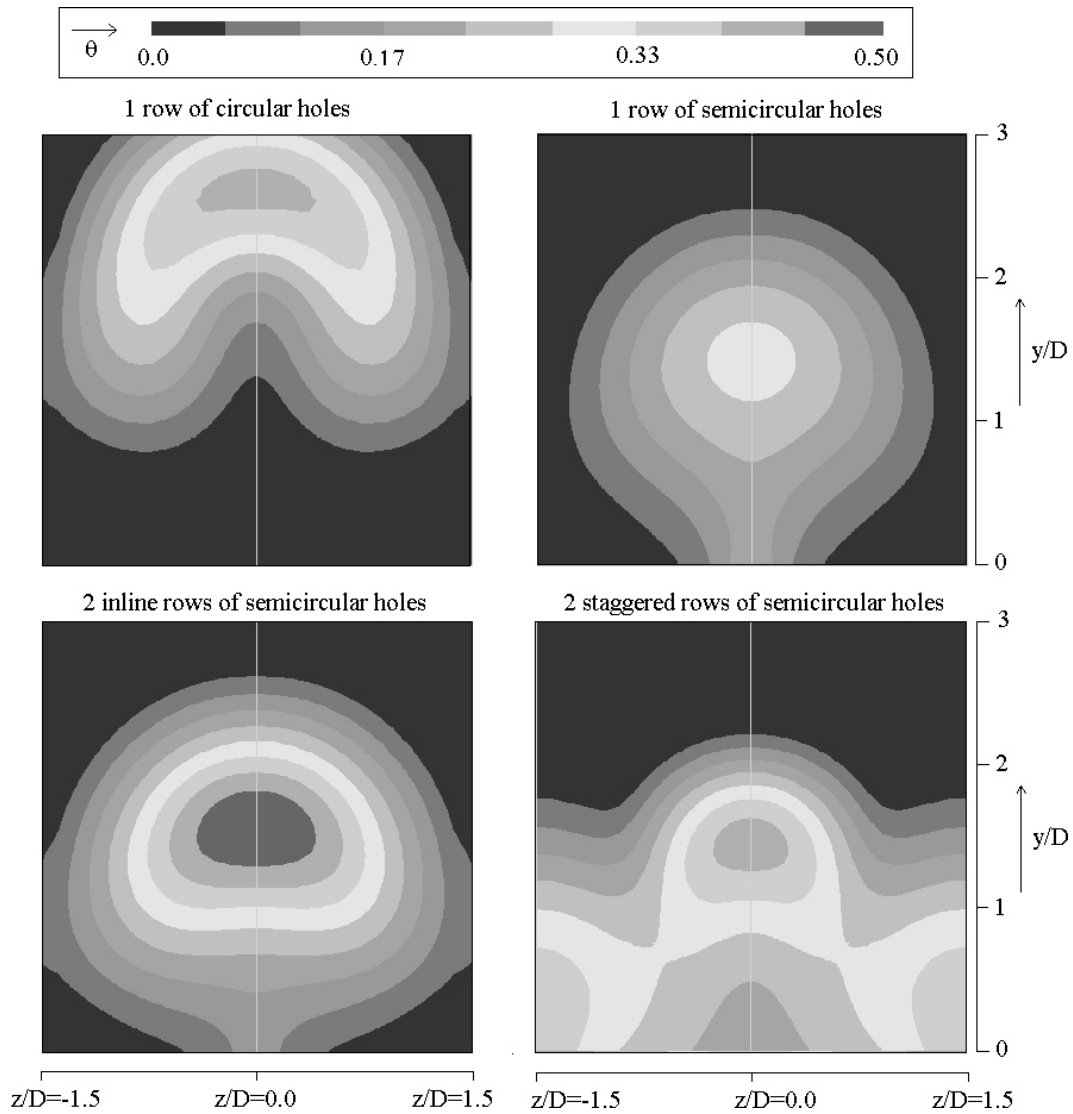


FIG. 14. NON-DIMENSIONAL TEMPERATURE CONTOURS AT PLANE $x/D=10.0$ AND AT $M=1.33$

T_{∞}	Mainstream Temperature
T_{aw}	Adiabatic Wall Temperature
T_c	Coolant Temperature
θ	Non-Dimensional Temperature
Wall Y^+	Mesh Dependent Dimensionless Distance
p	Pitch (Distance between Center of Holes in a Single Row)
s	Distance between Two Rows

Units

Velocity	Meter Per Second (m/sec)
Temperature	Melvin (K)
Length	Millimeters (mm)
Angle	Degree (o)
Pressure Atmospheric	(atm)

ACKNOWLEDGEMENT

This work is sponsored by Higher Education Commission, Pakistan under 5000 indigenous Ph.D. Scholarships program.

REFERENCES

- [1] Yuen, C.H.N., and Martinez-Botas, R.F., "Film Cooling Characteristics of a Single Round Hole at Various Streamwise Angles in a Crossflow: Part-I Effectiveness", *International Journal of Heat and Mass Transfer*, Volume 46, pp. 221-235, 2003.
- [2] Jung, I.S., and Lee, J.S., "Effect of Orientation Angles on Film Cooling Over a Flat Plate: Boundary Layer Temperature Distributions and Adiabatic Film Cooling Effectiveness", *Journal of Turbomachinery*, Volume 122, pp. 153-160, 2000.
- [3] Yuen, C.H.N., and Martinez-Botas, R.F., "Film Cooling Characteristics of Rows of Round Holes at Various Streamwise Angles in a Crossflow: Part-I. Effectiveness", *International Journal of Heat and Mass Transfer*, Volume 48, pp. 4995-5016, 2005.
- [4] Bernsdorf, S., Rose, M.G., and Abhari, R.S., "Modeling of Film Cooling Part-I: Experimental Study of Flow Structure", *Journal of Turbomachinery*, Volume 128, No.1, pp. 141-149, 2006.
- [5] Guo, T., and Li, S., "Numerical Simulation of Turbulent Jets with Lateral Injection into a Crossflow", *Journal of Hydrodynamics, Serial-B*, Volume 18, No. 3, pp. 319-323, 2006.
- [6] Hyder, M.J., and Asghar, F.H., "Effect of Coolant-to-Free-stream Velocity Ratios on Film Cooling Adiabatic Effectiveness for a Simple Planar Blade Test Section using FLUENT", *Proceedings of International Bhurban Conference on Applied Science and Technology Islamabad, Pakistan*, 8th-11th January, 2007.
- [7] Wang, T., and Li, X., "Mist Film Cooling Simulation at Gas Turbine Operating Conditions", *International Journal of Heat and Mass Transfer*, Volume 51 pp. 5305-5317, 2008.
- [8] Li, G., Zhu, H., and Fan, H., "Influences of Hole Shapes on Film Cooling Characteristics with CO₂ Injection", *Chinese Journal of Aeronautics*, Volume 21, pp. 393-401, 2008.
- [9] Yang, C., Lin, C.L., and Gau, C., "Film Cooling Performance and Heat Transfer over an Inclined Film-Cooled Surface at Different Divergent Angles with respect to Highly Turbulent Mainstream", *Experimental Thermal and Fluid Sciences*, Volume 32, pp. 1313-1321, 2008.
- [10] Rozati, A., and Tafti, D.K., "Effect of Coolant-Mainstream Blowing Ratio on Leading Edge Film Cooling Flow and Heat Transfer-LES Investigation", *International Journal of Heat and Fluid Flow*, Volume 29, pp. 857-873, 2008.
- [11] Lee, I., Chen, P., and Chyu, M.K., "An Experimental Investigation of Jet Flows through a Row of Forward Expanded Holes into a Mainstream Over a Concave Surface", *Experimental Thermal and Fluid Science*, Volume 32, pp. 1068-1080, 2008.
- [12] Jovanovic, M.B., deLange, H.C., and Van Steenhoven, A.A., "Effect of Hole Imperfection on Adiabatic Film Cooling Effectiveness", *International Journal of Heat and Fluid Flow*, Volume 29, pp. 377-386, 2008.
- [13] Pathak, M., Dass, A.K., and Dewan, A., "An Investigation of Turbulent Rectangular Jets Discharged into a Narrow Channel Weak Crossflow", *Journal of Hydrodynamics*, Volume 20, No. 2, pp. 154-163, 2008.
- [14] Liu, C., Zhu, H., and Bai, J., "Effect of Turbulent Prandtl Number on the Computation of Film-Cooling Effectiveness", *International Journal of Heat and Mass Transfer*, Volume 51, pp. 6208-6218, 2008.
- [15] Asghar, F.H., and Hyder, M.J., "Effect of Coolant to Free-stream Blowing Ratios and Boundary Layer Thickness on Film Cooling Adiabatic Effectiveness", *Proceedings of International Bhurban Conference on Applied Science & Technology Islamabad, Pakistan*, 19th -22nd January, 2009.
- [16] Asghar, F.H., and Hyder, M.J., "Computational Study of Film Cooling Effectiveness for a Comparison of Cylindrical, Square and Triangular Holes of Equal Cross-Sectional Area", *Mehran University Research Journal of Engineering & Technology*, 2009.
- [17] Yang, C., Lin, C.L., and Gau, C., "Film Cooling Performance and Heat Transfer Over an Inclined Film-Cooled Surface at Different Convergent Angles with Respect to Highly Turbulent Mainstream", *Applied Thermal Engineering*, Volume 29, pp. 167-177, 2009.
- [18] FLUENT 6.2 User's Guide. Fluent Incorporated, 2005.
- [19] Launder, B.E., and Spalding, D.B., "Lectures in Mathematical Models of Turbulence", Academic Press, London, England. 1974.
- [20] Zhang, X.Z., and Hassan, I., "Numerical Investigation of Heat Transfer on Film Cooling with Shaped Holes", *International Journal of Numerical Methods for Heat & Fluid Flow*, Volume 16, No. 8, pp. 848-869, 2006.
- [21] Barth, T.J., and Jespersen, D., "The Design and Application of Upwind Schemes on Unstructured Meshes", *Technical Report AIAA-89-0366*, AIAA 27th Aerospace Science Meeting, Reno, Nevada, 1989.
- [22] Rhie, C.M., and Chow, W.L., "Numerical Study of the Turbulent Flow Past an Airfoil with Trailing Edge Separation", *AIAA Journal*, Volume 21, No. 11, pp. 1525-1532, 1983.
- [23] Patankar, S.V., "Numerical Heat Transfer and Fluid Flow", Hemisphere Publishing Corporation, Washington, DC. 1980.